Journal of Intelligent Material Systems and Structures

In situ Strain and Temperature Monitoring of Adaptive Composite Materials
Hyuk-Jin Yoon, Daniele Marco Costantini, Hans Georg Limberger, René Paul Salathé, Chun-Gon Kim and Veronique Michaud

The online version of this article can be found at:

Published by:
⑤SAGE

Additional services and information for *Journal of Intelligent Material Systems and Structures* can be found at:

Email Alerts: http://jim.sagepub.com/cgi/alerts

Subscriptions: http://jim.sagepub.com/subscriptions

Reprints: http://www.sagepub.com/journalsReprints.nav

Permissions: http://www.sagepub.com/journalsPermissions.nav

Citations: http://jim.sagepub.com/content/17/12/1059.refs.html

>> Version of Record - Dec 5, 2006

What is This?

In situ Strain and Temperature Monitoring of Adaptive Composite Materials

Hyuk-Jin Yoon,[1] Daniele Marco Costantini,[2] Hans Georg Limberger,[2] René Paul Salathé,[2] Chun-Gon Kim[1] and Veronique Michaud[3],*

[1]*Smart Structures & Composites Laboratory, KAIST, Korea*

[2]*Advanced Photonics Laboratory, EPFL, Switzerland*

[3]*Laboratoire de Technologie des Composites et Polymères (LTC)*
Ecole Polytechnique Fédérale de Lausanne (EPFL), Switzerland

ABSTRACT: An optical fiber sensor is designed to simultaneously measure strain and temperature in an adaptive composite material. The sensor is formed by splicing two fiber Bragg gratings (FBGs) close to each other, which are written in optical fibers with different core dopants and concentrations. Their temperature sensitivities are hence different. The sensor is tested on an adaptive composite laminate made of unidirectional Kevlar-epoxy prepreg plies. Several 150 μm diameter prestrained NiTiCu shape memory alloy (SMA) wires are embedded in the composite laminate together with one fiber sensor. Simultaneous monitoring of strain and temperature during the curing process and activation in an oven is demonstrated.

Key Words: fiber Bragg grating, fiber sensor, adaptive composite, shape memory alloy, cure monitoring.

INTRODUCTION

WHEN considering the development of composite materials in the past 40 years, an evolution is clearly observed: the initial search was for very high specific properties alone, driven by aerospace application; the need to maintain high properties while reducing manufacturing time and production costs was then driven by automotive and other large scale applications; more recently, the desire to integrate additional functionality in the composite parts emerged. Since conventional structural composite materials cannot fulfill this last requirement alone, adaptive or smart composite materials, which integrate actuators and sensors, may hence well represent a next step in the development of composite materials. This evolution is driven in part by the need of automotive, sport or aerospace applications to gain efficiency not only by reducing structural weight, but also by directly integrating functions into the structure. Examples span from civil engineering where fiber optic sensors monitor bridges or dams (Bugaud et al., 2000), to sports equipments including skis or tennis rackets which are actively damped by piezo-electric fiber systems, to health monitoring or active

flutter reduction of airplanes (Balta et al., 2001a; Simpson and Boller, 2002). The evolution of composite materials is also driven by the fact that it is now possible to integrate both actuators and sensors directly into the composite material. Actuators and sensors have currently achieved a high enough degree of miniaturization not to disrupt the structural integrity of the composite part, both during processing and in service.

Fiber reinforced polymer composites containing thin shape memory alloy (SMA) wires as actuating elements (Wei et al., 1998a,b; Roytburd et al., 2000; Boller, 2001) represent an important class of 'smart materials'. The SMAs have been available for 40 years and have already found applications as actuators (Gandhi and Thompson, 1992), but they have only recently been manufactured as high quality wires with diameters below 0.2 mm. Thin SMA wires may be integrated in the host composite materials without affecting their integrity. In comparison to other actuating technologies, SMAs provide the following advantages: high reversible strains (up to 6%), high damping capacity, large reversible change of mechanical and physical characteristics, and most importantly, the ability to generate high recovery stresses. As a result, composite materials with SMA wires demonstrate added functional effects such as a shape change, a controlled overall thermal expansion or a shift in the natural vibration frequency

upon activation. The working principle is that prestrained martensitic SMAs tend to recover their initial shape when heated above their transformation temperature. If the wires alone are clamped externally or if they are embedded into a stiff host material, the wire strain recovery is limited, and instead large recovery stresses are generated, which may lead to the effects cited previously (Michaud et al., 2002; Schrooten et al., 2002a,b; Michaud, 2004).

The main drawback of these materials is that their transformation is induced by temperature, which greatly limits their response time controlled by heat transfer kinetics. Also, if a smart material is to be produced, it is necessary to locally monitor the strain and the temperature inside the structure. A sensor is thus needed, which is able to simultaneously measure strain and temperature and which can also be embedded into the host composite without modifying its properties and functions.

Currently, the most promising candidates are fiber optic sensors, which can be embedded in composite materials to locally measure strain, both during cure and during use (Measures, 1992; Hadjiprocopiou et al., 1996; Guemes and Menendez, 2002). In the last 10 years, researchers have been working on the principles and techniques to measure strain (e.g., by using fiber Bragg gratings, or other types of sensors such as Fabry-Perot cavities), temperature or other parameters such as humidity (Ferreira et al., 2000; Chi et al., 2001; Allsop et al., 2002; Kronenberg et al., 2002; Lai et al., 2002; Rao et al., 2002; Sivanesan et al., 2002; Shu et al., 2002; Frazao et al., 2003; Han et al., 2003). Moreover, the process of fiber embedding was investigated to ensure reliability and precision of the measurement (Measures, 1992; Bao et al., 2002; Guemes and Menendez, 2002). Combined with SMA actuators, as described earlier, optical fiber sensors have been shown to provide a composite with actuating and sensing capabilities for shape or stress control (Balta et al., 2005; Yoon et al. 2005).

However, the use of fiber Bragg grating (FBG) sensors is limited by their simultaneous dependence on strain and temperature. In a previous work (Balta et al., 2005), a thermocouple was pasted on the structure to monitor the temperature and back-calculate the strain. To overcome this cross sensitivity using only embedded optical fibers, a number of techniques have been proposed, most of them relying on the deconvolution of two simultaneous measurements. These methods include the dual-wavelength superimposed gratings (Xu et al., 1994), the use of first- and second-order diffraction grating wavelengths (Echevarria et al., 2001), FBGs in optical fibers with different dopants (Cavaleiro et al., 1999; Guan et al., 2000), hybrid Bragg grating/long period gratings (Patrick et al., 1996), dual-diameter FBGs (James et al., 1996), FBGs combined with EDFAs

(Jung et al., 1999), FBG/EFPI combined sensors (Zeng and Rao, 2001; Kang et al., 2003), FBGs in high-birefringence optical fibers (Ferreira et al., 2000), the employment of strain-free FBGs (Song et al., 1997; Guan et al., 2002), and a combination of FBGs of different 'type' (Shu et al., 2002; Frazao et al., 2003). The use of a strain-free reference grating turns out to be the most efficient way to discriminate strain and temperature. On the other hand, it is not easy to implement this technique when sensors must be embedded into a host composite, since it requires placing a grating into a small capillary tube or another envelop protecting it from strain.

In the present article, a method to simultaneously monitor the strain and temperature in an adaptive composite laminate using a FBG-based sensor has been proposed. The technique relying on the combination of the two FBGs written in optical fibers with different core dopants was improved for the present application. A suitable couple of optical fibers were selected, and their respective temperature and strain sensitivities were measured before integration. Finally, strain and temperature inside a Kevlar epoxy composite laminate with SMA wires were measured during curing and activation, to demonstrate the operation of the fiber sensor.

SENSOR DEVELOPMENT

Principle

A fiber Bragg grating consists of a periodic change of the core refractive index of an optical fiber and reflects light around the resonance peak wavelength defined by the following phase matching condition:

$$\lambda_B = 2n_e \Lambda \tag{1}$$

where λ_B is the Bragg wavelength, n_e is the core effective refractive index, and Λ is the period of the grating. The shift of the Bragg wavelength $\Delta\lambda_B$ due to a temperature change ΔT and an external axial strain ε can be expressed for a bare fiber Bragg grating, which is neither bonded nor embedded, as:

$$\Delta\lambda_B = \lambda_B[(\alpha + \xi)\Delta T + (1 - p_e)\varepsilon]. \tag{2}$$

where α is the coefficient of thermal expansion of the fiber material, ξ is the thermooptic coefficient and p_e is the strain-optic constant (Kersey et al., 1997). The relative Bragg wavelength shift $\Delta\lambda_B/\lambda_B$ may simply be written as a function of the temperature sensitivity $K_T = \alpha + \xi$ and the strain sensitivity $K_\varepsilon = 1 - p_\varepsilon$ of the fiber Bragg grating:

$$\frac{\Delta\lambda_B}{\lambda_B} = K_T\Delta T + K_\varepsilon\Delta\varepsilon. \tag{3}$$

It is assumed that the thermal and applied strain responses of the grating are independent. This has been shown to be valid, if the sensing length is not too long, or the temperature and strain variations are not too large. Otherwise, cross-sensitivity terms need to be taken into account (Farahi et al., 1990). In this work, this assumption has been adopted, as the temperature variation does not exceed $120°C$, and the strain is lower than 10^{-3}. The response of the two fiber Bragg gratings having different temperatures and/or strain sensitivities can be combined into a linear system of two equations, which can be solved to obtain simultaneously the temperature change and strain:

$$\begin{bmatrix} \Delta T \\ \varepsilon \end{bmatrix} = \begin{bmatrix} K_{T1} & K_{\varepsilon 1} \\ K_{T2} & K_{\varepsilon 2} \end{bmatrix}^{-1} \begin{bmatrix} \dfrac{\Delta \lambda_{B1}}{\lambda_{B1}} \\ \dfrac{\Delta \lambda_{B2}}{\lambda_{B2}} \end{bmatrix} = K^{-1} y. \qquad (4)$$

where the subscripts 1, 2 indicate the specific FBGs, K is the 2×2 matrix of the coefficients, and y is the vector of relative wavelength shifts. Equation (4) can be written in vector form as $x = K^{-1} y$, where x is the vector formed by the temperature and strain components. In order to efficiently discriminate the temperature and the strain contributions, the matrix of coefficients K must be well-conditioned (Sivanesan et al., 2002). The relative error δx in temperature and strain is related to the Bragg wavelength change vector δy as follows:

$$\frac{\|\delta x\|}{\|x\|} \leq C(K) \frac{\|\delta y\|}{\|y\|}. \qquad (5)$$

where $C(K) = \|K\| \|K^{-1}\|$ is the condition number of the matrix of coefficients K (Strang, 1988). In order to reduce the error in the simultaneous evaluation of strain and temperature, a small condition number is desired.

Fiber Sensor Design

The thermooptic coefficient of an optical fiber depends on the core dopants and their relative concentrations (Cavaleiro et al., 1999; Guan et al., 2000; Oh et al., 2000). Based on this principle, a panel of fibers, with different core dopants and concentrations, was investigated, in order to select a couple that provided a low condition number. Two fiber Bragg gratings, one written in each fiber, and spliced to each other as shown in Figure 1 formed the strain and temperature sensor. The fiber specifications and the fabrication parameters are listed in Table 1. The gratings were fabricated in these optical fibers with the phase-mask technique using a 193 nm ArF excimer laser. The same phase mask with a period of 1058.5 nm was used. The length of the FBG was of 7 mm and their reflectivity was around 50%. Since the maximum curing temperature of the Kevlar epoxy composite material is of $140°C$, the FBG sensors were pre-annealed at $160°C$ during
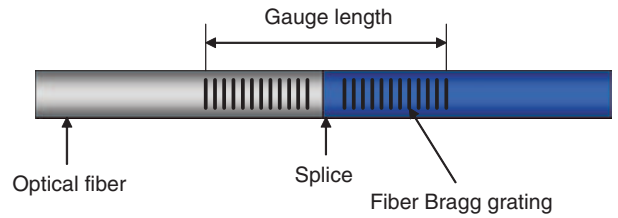

Figure 1. *Design of the FBG-based sensor to simultaneously measure temperature and strain.*

Table 1. Fiber Bragg gratings fabrication parameters (core dopants and concentrations as provided by the manufacturer, F_P: fluence per pulse, F_T: total fluence and λ_B: Bragg wavelength).

Fiber label	Fiber supplier	Core dopants GeO$_2$	B$_2$O$_3$ (mol%)	F_P (mJ/cm^2)	F_T (J/cm^2)	λ_B (nm)
SMF-28e	Corning	$\sim$3	–	90.9	4080	1532
G9	Cabloptic	9	–	150	230	1532
G18	Cabloptic	18	–	68.8	26.68	1536
G22	CSEM	22	–	68.8	1.1	1547
G25	CSEM	25	–	68.8	1.31	1551
PS1500	Fibercore	10	14–18	68.8	5.5	1532
Photosil	Spectran	$\sim$30	Unknown	100	58.1	1531

48 h, in order to ensure the Bragg wavelength stability (Kannan et al., 1997).

The temperature and strain sensitivities of the gratings were separately measured. The wavelength shift of the Bragg gratings as a function of temperature was measured in reflection with a wavelength resolution of 0.1 pm by a tunable laser (Tunics 1550, Nettest), a photo-detector (MA9305B, Anritsu), and a wavelength meter (WA-1500, EXFO Burleigh). The relative wavelength shifts were acquired for each Bragg grating by increasing the temperature from 20 to $150°C$ in increments of $10°C$. Each grating was heated in an oven and the temperature was measured with a resolution of $\pm 0.1°C$ by a thermocouple connected to a voltmeter (FLUKE 52 k/J). The temperature sensitivities of the FBGs calculated with the linear fit are listed in Table 2. The thermal expansion coefficient of the fiber material is nearly of an order of magnitude lower than the thermooptic coefficient (Jewell et al., 1991). Thus the temperature sensitivity is mainly affected by the thermooptic coefficient, which, in turn, depends on the concentrations of GeO$_2$ and B$_2$O$_3$ in the core. This explains the difference in temperature sensitivity of the gratings written in the GeO$_2$ series and GeO$_2$-B$_2$O$_3$ co-doped silica fibers, and the higher temperature sensitivity with increasing GeO$_2$ concentration. The G22 and PS1500 fibers which exhibit a large difference in temperature sensitivity were selected as the combination of fibers for the strain–temperature sensor. The G25 fiber was not selected because its cladding was 80 µm in
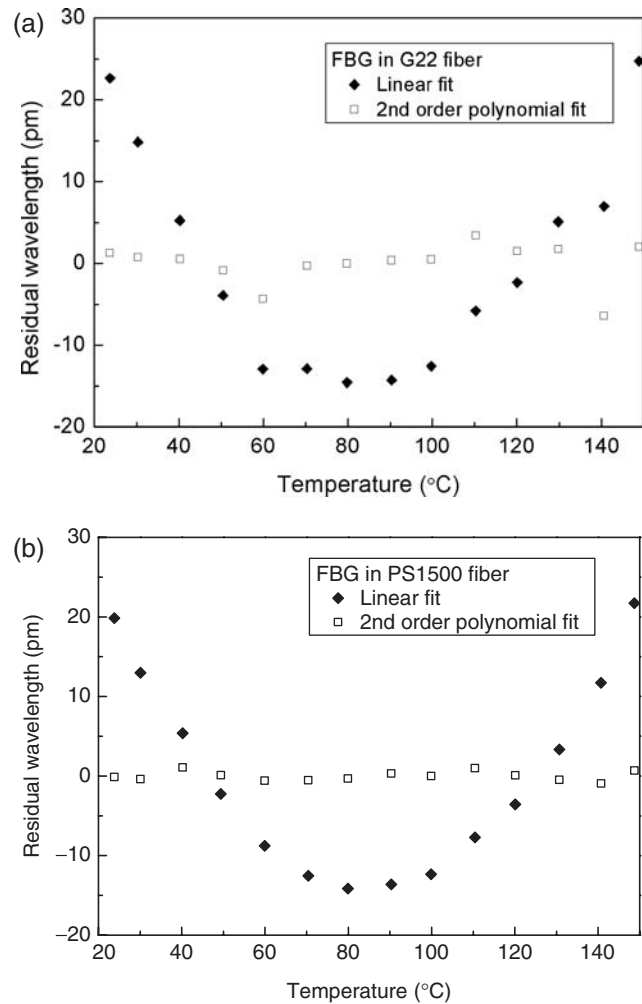
Table 2. Temperature sensitivities of FBGs.

Fiber label	K_T ($10^{-6\circ}C^{-1}$)
SMF-28e	6.92 ± 0.02
G9	6.97 ± 0.02
G18	7.19 ± 0.02
G22	7.48 ± 0.02
G25	7.60 ± 0.02
PS1500	6.00 ± 0.01
Photosil	6.39 ± 0.02
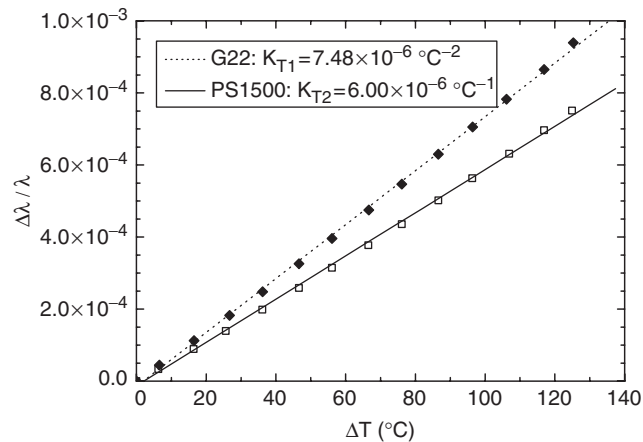
Figure 2. Relative Bragg wavelength shift versus temperature change for both the gratings written in the G22 and PS1500 optical fibers.

Figure 3. Residual wavelength shift for linear and second-order polynomial fit as a function of temperature change for both gratings written: (a) in the G22 and (b) in the PS1500 optical fibers.
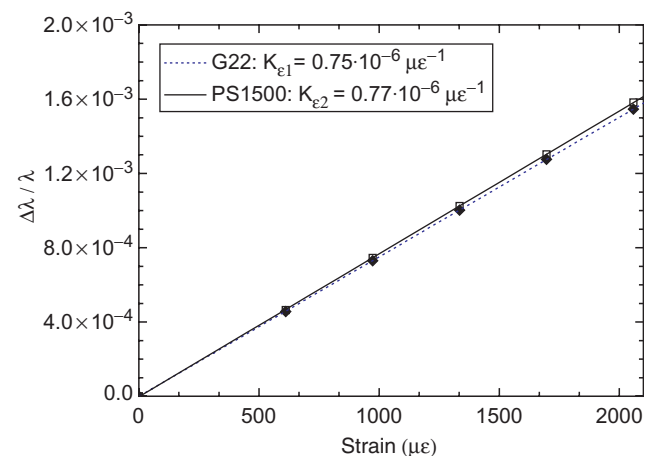
Figure 4. Relative Bragg wavelength shift versus applied strain for both the gratings written in the G22 and PS1500 optical fibers.

diameter, and slightly elliptic, which prevented to ensure a reproducible splicing operation.

The solid and dotted lines in Figure 2 represent the linear fitting to the experimental data for the G22 and PS1500 fibers, respectively. The G22 fiber has a temperature coefficient K_{T1} of $7.48 \pm 0.02 \times 10^{-6\circ}C^{-1}$, while the PS1500 has a coefficient K_{T2} of $6.00 \pm 0.01 \times 10^{-6\circ}C^{-1}$. A deviation from linearity is observed in the figure, and the response of the FBGs is shown to rather follow a quadratic behavior. The residual wavelength difference for the linear and the second-order polynomial fits are given in Figure 3. This nonlinear temperature response was already modeled by Ghosh (Ghosh, 1995; Pal et al., 2004). However, in order to use Equation (4) for a simultaneous recovering of strain and temperature, the temperature response of the sensors was fitted to a linear curve, which can lead to a maximum error of 1.3% in the temperature range of operation of 20–150°C.

Figure 4 shows the relative Bragg wavelength change for the two gratings when the applied strain is between 0 and 2000 µε. The strain was induced by suspending the calibrated weights to the optical fiber, and assuming for the silica fiber a Young modulus of 72.5 GPa (Kersey et al., 1997) and a cladding diameter of 125 µm. The experimental data obtained for the G22

and PS1500 grating sensors were linearly fitted. Their strain sensitivities were similar and equal to $0.75 \pm 0.01 \times 10^{-6}$ µε^{-1} and $0.77 \pm 0.01 \times 10^{-6}$ µε^{-1}, respectively.

Table 3. Condition numbers of dual FBG sensors.

Fiber 1			Fiber 2				
	K_{T1} ($10^{-6\circ}C^{-1}$)	$K_{\varepsilon1}$ ($10^{-6}\mu\varepsilon^{-1}$)		K_{T2} ($10^{-6\circ}C^{-1}$)	$K_{\varepsilon2}$ ($10^{-6}\mu\varepsilon^{-1}$)	$C(K)$	Ref.
Siecor SMF1528	6.48 ± 0.02	0.745 ± 0.002	Fibercore PS1500	5.76 ± 0.03	0.741 ± 0.002	147.9	Cavaleiro et al., 1999
Corning SMF-28	6.85	0.68	Er/Yb co-doped	5.93	0.67	146.1	Guan et al., 2000
B/Ge co-doped fiber (Type IA grating)	4.74	0.69	B/Ge co-doped fiber (Type IIA grating)	6.45	0.69	55.3	Shu et al., 2002
Fibercore SM1500 (Type I grating)	7.820 ± 0.006	0.74 ± 0.05	Fibercore SM1500 (Type IIA grating)	8.700 ± 0.006	0.750 ± 0.006	240.7	Frazao et al., 2003
CSEM G22	7.48 ± 0.02	0.75 ± 0.01	Fibercore PS1500	6.00 ± 0.01	0.77 ± 0.01	73.8	This work

The condition number of this FBG couple was calculated and is compared in Table 3 to that obtained using similar methods found in literature. The fiber couple from this work is very promising in terms of accuracy to simultaneously discriminate the temperature and strain: the condition number was improved by about 50% when compared to similar techniques and is similar to that of the sensors combining Bragg gratings of different 'types' (Shu et al., 2002).

CURING AND ACTIVATION MONITORING OF AN ADAPTIVE COMPOSITE

Composite Material and Embedding Procedures

The sensor previously described was embedded in an adaptive composite laminate to validate the *in situ* simultaneous monitoring of strain and temperature. The base composite was an unidirectional laminate made from Kevlar 29 aramid fibers and LTM217 epoxy resin prepreg (Advanced Composites Group, UK), with about 60% volume fraction fibers. The wires were NiTiCu SMA (Furukawa, Japan) with a diameter of 150 μm. These wires were in martensitic phase at room temperature, and transform to austenite with the respective transformation temperatures: austenite start, $A_s = 52.3^\circ C$, austenite finish, $A_f = 77.7^\circ C$, martensite start, $M_s = 34.9^\circ C$ and martensite finish $M_f = -20^\circ C$. These wires were chosen since they exhibit very low hysteresis and a recovery force which increases almost linearly with temperature, reaching about 650 MPa at 100°C when prestrained by 3% (Michaud and Månson, 2004).

An adaptive composite was produced according to the configuration given in Figure 5. Two layers of Kevlar-epoxy prepreg were placed on an aluminum base plate. Eight shape memory wires were laid on the neutral axis of the specimen, spaced every millimeter, together with the FBG sensor in the center. Another two layers of Kevlar-epoxy prepreg were then laid on the top so as to keep the wires and sensor in the neutral axis of the specimen. The SMA wires were maintained in a frame, and prestrained to 3%. The prestrain was maintained during the curing process. Details on the processing of the adaptive composites are given in references (Balta et al., 2001b; Michaud and Månson, 2004). The whole assembly was then placed in a vacuum bag, and maintained under vacuum during the composite cure and post-cure. A thermocouple was attached to the bag surface close to the sample in order to have a reference temperature.

RESULTS AND DISCUSSION

The sensor was first used to monitor the temperature and strain in the material during curing. The experimental setup for cure monitoring is described in Figure 6. The light from the polarized tunable laser was passed through a polarization scrambler to eliminate any birefringence effect of the Bragg gratings on the spectral response. In addition, the tunable laser light wavelength was continuously calibrated using a wavelength meter, with a resolution of 0.1 pm. The wavelength of the light-source, the light intensity reflected by the sensor, and the temperature measured by the thermocouple were acquired by a computer controlled data acquisition system.

The composite laminate sample was placed in the autoclave and cured according to the LTM217 epoxy resin cycle. The temperature was increased from room temperature to 70°C with a rate of 4°C/min and maintained constant for 12 h. After the first dwell, the temperature was increased to 140°C and the heating rate was set to 20°C/h. After the second dwell, the temperature was lowered back to room temperature. The total cure cycle was of 24 h. During curing both the internal strain and the temperature were computed simultaneously according to Equation (4), as shown in Figure 7.

At the beginning of the curing process, there was no strain and the room temperature was of 27°C. After closing the autoclave, the temperature was increased to 70°C in 1 h. In this time interval, the temperature and the strain could not be measured by the FBG sensor, because the changes were too fast for the interrogation system to follow. Indeed, 14 min were required to
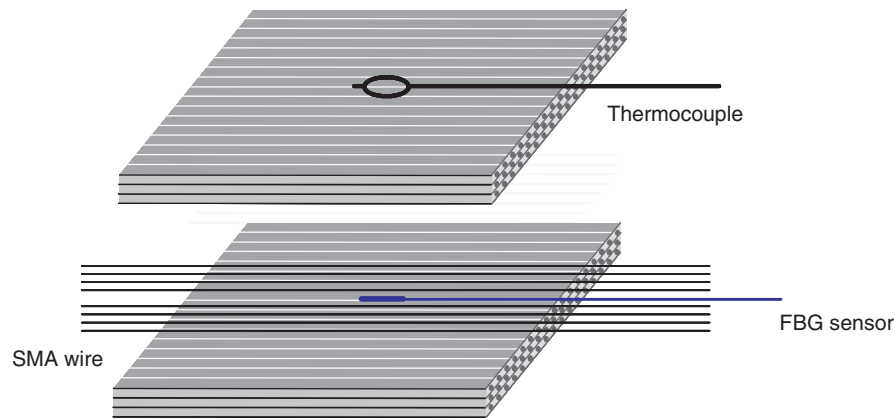
Figure 5. *Direction and location of FBG and SMA wires into the composite laminate.*
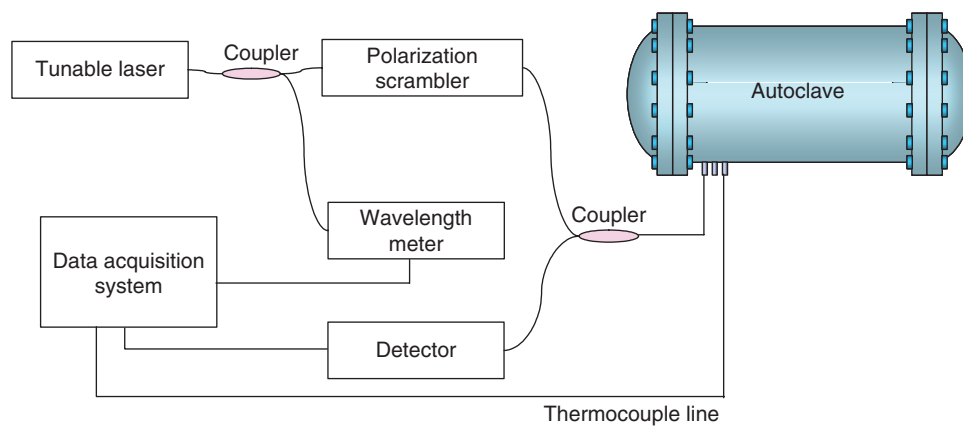

Figure 6. *The experimental setup for the cure monitoring of the composite laminate.*
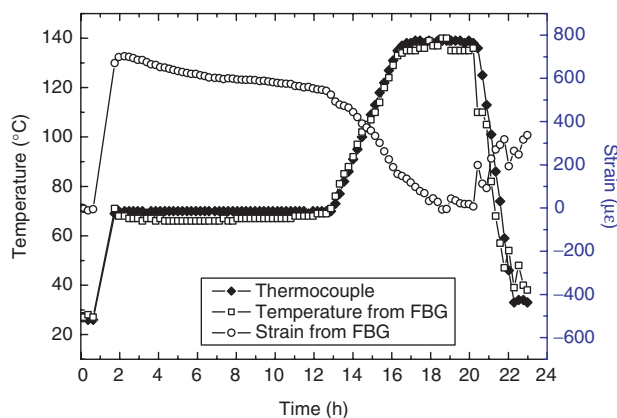

Figure 7. *Strain and temperature measured within the laminate by the FBG sensor as a function of time. The thermocouple signal is also shown as a reference.*

acquire a FBG sensor spectrum due to the low scanning speed of the laser/wavelength meter system over the gratings wavelength range. During the dwell, the strain was positive in the composite because the thermal expansion of the aluminum base-plate (corresponding to about $1000\,\mu\varepsilon$) was partially transferred to the composite. Then the strain decreased as a result of the polymer cross-linking. During the second heating ramp, the strain further decreased since the thermal expansion coefficient of the Kevlar-epoxy composite is negative, which is about $-3 \times 10^{-6}/K$. In the post-curing phase, the strain decreased because of the polymer cross-linking. Finally, in the cooling down phase the composite expanded due to its negative thermal expansion coefficient. After the curing process, the residual internal strain was of $340\,\mu\varepsilon$. The results are consistent with those found earlier with a simple Bragg grating sensor (Balta et al., 2005), but it is also shown that the cure schedule (direct heating to $140°C$ after the first dwell at $70°C$, or a cooling-down step in between) exerts a significant influence on the final value of strain within the composite. The fiber optic sensor is in tension after the present cure schedule, whereas it was found to be in compression ($-800\,\mu\varepsilon$) after the cure schedule comprising a cool-down stage in between the two temperature dwells.

The temperature measurement from the FBG sensor followed the thermocouple values within 6%. The thermocouple was placed on the surface of the sample while the fiber sensor was embedded inside the laminate.
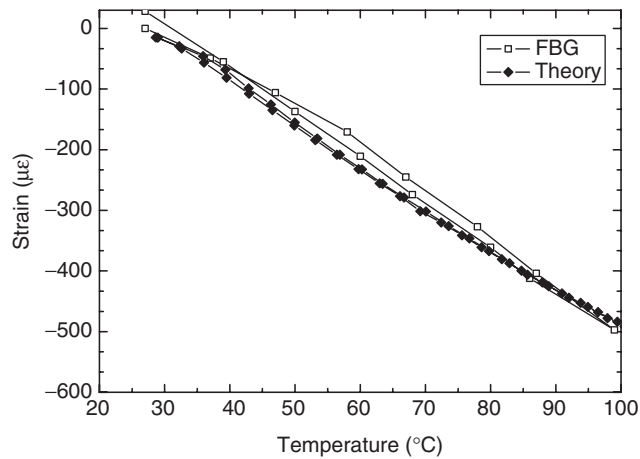
Figure 8. *Thermal activation of the adaptive composite specimen: strain measured by the FBG sensor (open squares) and strain predicted by theory, Equation (6) (diamonds), as a function of temperature.*

This can result in a small temperature difference and can add some uncertainties to the maximum experimental errors of $\pm 22.1\,\mu\varepsilon$ and $\pm 2.4^{\circ}C$ calculated for the FBG sensor using Equations (11) and (12) from Sivanesan et al., 2002.

After the curing process, the sample was demolded. Activation of the SMA wires was then performed by heating the composite sample in an oven up to $100^{\circ}C$. Figure 8 shows the recovery strain in the composite measured by the FBG sensor. As expected, the composite contracted when heated due to the combined effects of the negative thermal expansion and the recovery of the SMA wires above their transformation temperature.

In order to validate the sensor reading, the experimental values were compared to the theoretical predictions. The composite strain was obtained by a simple force balance, such that

$$\varepsilon_{\text{comp}}(\sigma, T) = \frac{\sigma_{\text{m}}}{E_{\text{c}}} - \alpha_{\text{c}}(T - T_{\text{rs}}) \qquad (6)$$

where T_{rs} is the temperature at which the constrained thermal load starts, α_{c} the CTE of the host composite, E_{c} the Young's modulus of the host composite, and σ_{m} the stress in the host composite. The latter is related to the stress exerted by a wire σ_{w}, and is calculated at each step using a direct fit to the recovery force behavior of a single wire, as follows:

$$\sigma_{\text{m}} = -\frac{V_f}{1 - V_f}\sigma_{\text{w}} \qquad (7)$$

where V_{f} is the wire volume fraction. Finally, the modulus of the entire composite is written with a rule of mixtures from the moduli of the host composite and wire as:

$$E_{\text{comp}} = V_{\text{f}}E_{\text{w}} + (1 - V_{\text{f}})E_{\text{c}} \qquad (8)$$

The matrix modulus, E_{c} is considered to be temperature independent in a first approximation, while the Young's modulus of the wire, E_{w}, is temperature dependent and hysteretic (Michaud et al., 2002; Michaud and Månson, 2004). In the present case, the SMA wire volume fraction V_{f} was 1.7%, and for the other materials, values were taken as in reference (Michaud and Månson, 2004). This simple model was shown to provide very good results for this type of activation in unidirectional composites (Michaud and Månson, 2004). The model predictions are shown on Figure 5 together with the experimental results. The theoretical and experimental data are in good agreement, indicating that the sensor developed in this work is able to accurately monitor both temperature and strain in real time during activation of the composite with embedded SMA wires.

CONCLUSION

A sensor suitable for the simultaneous measurement of strain and temperature within a host composite material has been realized and tested. The sensor is formed by two FBGs, which are written in optical fibers with different dopants in the core. A sensing element results with two Bragg gratings having peak wavelengths around 1550 nm of similar strain sensitivity but different response to temperature. The FBGs in a germanosilicate fiber with 22 mol% GeO_2 and in a fibercore PS1500 germanium-boron co-doped fiber were selected for building this sensing element. The temperature coefficients were different by 25%, resulting in an improved condition number with respect to similar sensors.

Strain and temperature of a Kevlar epoxy adaptive composite, in which several 150 μm diameter NiTiCu SMA wires were embedded, were measured simultaneously using an embedded FBG sensor during the cure cycle. Finally, activation tests were performed on the composites by placing them in an oven up to $100^{\circ}C$, and monitoring the strain and temperature. The composite contracted upon heating due to the recovery of the SMA wires above the transformation temperature. The experimental strain–temperature curve was compared well with an elastic force balance analysis. A 'smart' material was thus produced, which can readily be used in applications such as strain control, shape change or resonance frequency shift.

the Swiss–Korean collaboration program. Initial developments of the adaptive composites were performed in the frame of the ADAPT Brite/EuRam Project, supported the European Commission and the Swiss Federal Education and Science Office for the Swiss partners.

REFERENCES

Allsop, T., Zhang, L., Webb, D.J. and Bennion, I. 2002. "Discrimination between Strain and Temperature Effects using First and Second-order Diffraction from a Long-period Grating," *Optics Communications*, 211(1/6):103–108.

Balta, J.A., Simpson, J., Michaud, V., Månson, J.A.-E. and Schrooten, J. 2001a. "Embedded Shape Memory Alloys Confer Aerodynamic Profile Adaptivity," *Smart Materials Bulletin*, 12:8–12.

Balta, J.A., Michaud, V., Parlinska, M., Gotthardt, R. and Månson, J.A.-E. 2001b. "Adaptive Composites with Embedded NiTiCu Wires," In: *Proceedings of SPIE*, 4333, *Smart Structures and Materials 2001*, pp. 377–386.

Balta, J.A., Bosia, F., Michaud, V., Dunkel, G., Botsis, J. and Månson, J.A.-E. 2005. "Smart Composites with Embedded Shape Memory Alloy Actuators and Fibre Bragg Grating Sensors: Activation and Control," *Smart Materials and Structures*, 14(4):457–465.

Bao, X., Huang, C., Zeng, X., Arcand, A. and Sullivan, P. 2002. "Simultaneous Strain and Temperature Monitoring of the Composite Cure with a Brillouin-scattering-based Distributed Sensor," *Optical Engineering*, 41(7):1496–1501.

Boller, C. 2001. *The Encyclopedia of Materials: Science and Technology*, Elsevier Science Ltd.

Bugaud, M., Ferdinand, P., Rougeault, S., Dewynter-Marty, V., Parneix, P. and Lucas, D. 2000. "Health Monitoring of Composite Plastic Waterworks Lock Gates using In-fibre Bragg Grating Sensors," *Smart Materials and Structures*, 9(3):322–327.

Cavaleiro, P.M., Araujo, F.M., Ferreira, L.A., Santos, J.L. and Farahi, F. 1999. "Simultaneous Measurement of Strain and Temperature using Bragg Gratings Written in Germanosilicate and Boron-codoped Germanosilicate Fibers," *IEEE Photonics Technology Letters*, 11(12):1635–1637.

Chi, H., Tao, X.M., Yang, D.X. and Chen, K.S. 2001. "Simultaneous Measurement of Axial Strain, Temperature, and Transverse Load by a Superstructure Fiber Grating," *Optics Letters*, 26(24):1949–1951.

Echevarria, J., Quintela, A., Jauregui, C. and Lopez-Higuera, J.M. 2001. "Uniform Fiber Bragg Grating First- and Second-order Diffraction Wavelength Experimental Characterization for Strain-temperature Discrimination," *IEEE Photonics Technology Letters*, 13(7):696–698.

Farahi, F., Webb, D.J., Jones, J.D.C. and Jackson, D.A. 1990. "Simultaneous Measurement of Temperature and Strain: Cross-sensitivity Considerations," *Journal of Lightwave Technology*, 8(2):138–142.

Ferreira, L.A., Araujo, F.M., Santos, J.L. and Farahi, F. 2000. "Simultaneous Measurement of Strain and Temperature using Interferometrically Interrogated Fiber Bragg Grating Sensors," *Optical Engineering*, 39(8):2226–2234.

Frazao, O., Lima, M.J.N. and Santos, J.L. 2003. "Simultaneous Measurement of Strain and Temperature using Type I and Type IIA Fibre Bragg Gratings," *Journal of Optics A-Pure Applied Optics*, 5(3):183–185.

Gandhi, M.V. and Thompson, B.S. 1992. *Smart Materials and Structures*, Chapman & Hall.

Ghosh, G. 1995. "Model for the Thermo-optic Coefficients of Some Standard Optical Glasses," *Journal of Non-crystalline Solids*, 189:191–196.

Guan, B.O., Tam, H.Y., Ho, S.L., Chung, W.H. and Dong, X.Y. 2000. "Simultaneous Strain and Temperature Measurement using a Single Fibre Bragg Grating," *Electronics Letters*, 36(12):1018–1019.

Guan, B.O., Tam, H.Y., Chan, H.L.W., Choy, C.L. and Demokan, M.S. 2002. "Discrimination between Strain and Temperature with a Single Fiber Bragg Grating," *Microwave and Optical Technology Letters*, 33(3):200–202.

Guemes, J.A. and Menendez, J.M. 2002. "Response of Bragg Grating Fiber-optic Sensors when Embedded in Composite Laminates," *Composite Science and Technology*, 62(7/8):959–966.

Hadjiprocopiou, M., Reed, G.T., Hollaway, L. and Thorne, A.M. 1996. "Optimization of Fibre Coating Properties for Fiber Optic Smart Structures," *Smart Materials and Structures*, 5(4):441–448.

Han, Y.G., Lee, S.B., Kim, C.S., Kang, J.U., Paek, U.C. and Chung, Y. 2003. "Simultaneous Measurement of Temperature and Strain using Dual Long-period Fiber Gratings with Controlled Temperature and Strain Sensitivities," *Optics Express*, 11(5):476–481.

James, S.W., Dockney, M.L. and Tatam, R.P. 1996. "Simultaneous Independent Temperature and Strain Measurement using In-fibre Bragg Grating Sensors," *Electronics Letters*, 32(12):1133–1134.

Jewell, J.M., Askins, C.G. and Aggarwal, I.D. 1991. "Interferometric Method for Concurrent Measurement of Thermo-optic and Thermal Expansion Coefficients," *Applied Optics*, 30(25):3656–3660.

Jung, J., Nam, H., Lee, J.H., Park, N. and Lee, B. 1999. "Simultaneous Measurement of Strain and Temperature by Use of a Single-fiber Bragg Grating and an Erbium-doped Fiber Amplifier," *Applied Optics*, 38(13):2749–2751.

Kang, H.K., Kang, D.H., Hong, C.S. and Kim, C.G. 2003. "Simultaneous Monitoring of Strain and Temperature during and after Cure of Unsymmetric Composite Laminate using Fibre-optic Sensors," *Smart Materials and Structures*, 12(1):29–35.

Kannan, S., Guo, J.Z.Y. and Lemaire, P.J. 1997. "Thermal Stability Analysis of UV-induced Fiber Bragg Gratings," *Journal of Lightwave Technology*, 15(8):1478–1483.

Kersey, A.D., Davis, M.A., Patrick, H.J., LeBlanc, M., Koo, K.P., Askins, C.G., Putnam, M.A. and Friebele, E.J. 1997. "Fiber Grating Sensors," *Journal of Lightwave Technology*, 15(8):1442–1463.

Kronenberg, P., Rastogi, P.K., Giaccari, P. and Limberger, H.G. 2002. "Relative Humidity Sensor with Optical Fiber Bragg Gratings," *Optics Letters*, 27(16):1385–1387.

Lai, Y.C., Qiu, G.F., Zhang, W., Zhang, L., Bennion, I. and Grattan, K.T.V. 2002. "Amplified Spontaneous Emission-based Technique for Simultaneous Measurement of Temperature and Strain by Combining Active Fiber with Fiber Gratings," *Review of Scientific Instruments*, 73(9):3369–3372.

Measures, R.M. 1992. "Smart Composite Structures with Embedded Sensors," *Composites Engineering*, 2(5/7):597–618.

Michaud, V. 2004. "Can Shape Memory Alloy Composites be Smart?," *Scripta Materialia*, 50(2):249–253.

Michaud, V., Schrooten, J., Parlinska, M., Gotthardt, R. and Bidaux, J.E. 2002. "Shape Memory Alloy Wires Turn Composites into Smart Structures. Part II: Manufacturing and Properties," In: *Proceedings of SPIE 4698*, *Smart Structures and Materials 2002*, pp. 406–415.

Michaud, V. and Månson, J.-A.E. 2004. "Progress and Design of Composites with Embedded Shape Memory Alloy Wires," *Transactions of the Materials Research Society of Japan*, 29(7):3043–3048.

Oh, K., Han, Y.G., Seo, H.S., Chung, Y., Paek, U.C., Jang, J.N. and Kim, M.S. 2000. "Compositional Dependence of the Temperature Sensitivity in a Long Period Grating Imprinted on GeO$_2$-B$_2$O$_3$ Co-doped Core Silica Fibers," *OSA Trends in Optics and Photonics*, pp. 243–248.

Pal, S., Sun, T., Grattan, K.T.V., Wade, S.A., Collins, S.F., Baxter, G.W., Dussardier, B. and Monnom, G. 2004. "Non-linear Temperature Dependence of Bragg Grating Written in

Different Fibres, Optimized for Sensor Applications over a Wide Range of Temperatures,'' *Sensors and Actuators*, 112(2/3):211–219.

Patrick, H.J., Williams, G.M., Kersey, A.D., Pedrazzani, J.R. and Vengsarkar, A.M. 1996. ''Hybrid Fiber Bragg Grating/Long Period Fiber Grating Sensor for Strain/Temperature Discrimination,'' *IEEE Photonics Technology Letters*, 8(9):1223–1225.

Rao, Y.J., Yuan, S.F., Zeng, X.K., Lian, D.K., Zhu, Y., Wang, Y.P., Huang, S.L., Liu, T.Y., Fernando, G.F., Zhang, L. and Bennion, I. 2002. ''Simultaneous Strain and Temperature Measurement of Advanced 3-D Braided Composite Materials using an Improved EFPI/FBG System,'' *Optics and Lasers in Engineering*, 38(6):557–566.

Roytburd, A.L., Slutsker, J. and Wuttig, M. 2000. *Comprehensive Composite Materials*, 5, Elsevier.

Schrooten, J., Michaud, V., Parthenios, J., Psarras, G.C., Galiotis, C., Gotthardt, R., Månson, J.-A.E. and Van Humbeeck, J. 2002a. ''Progress on Composites with Embedded Shape Memory Alloy Wires,'' *Materials Transactions*, 43(5):961–973.

Schrooten, J., Michaud, V., Zheng, Y., Balta, J.A. and Månson, J.-A.E. 2002b. ''Shape Memory Alloy Wires Turn Composites into Smart Structures: Part I. Material Requirements,'' In: *Proceedings of SPIE 4698, Smart Structures and Materials 2002*, pp. 395–405.

Shu, X., Liu, Y., Zhao, D., Gwandu, B., Floreani, F., Zhang, L. and Bennion, I. 2002. ''Dependence of Temperature and Strain Coefficients on Fiber Grating Type and its Application to Simultaneous Temperature and Strain Measurement,'' *Optics Letters*, 27(9):701–703.

Simpson, J. and Boller, C. 2002. ''Performance of SMA-reinforced Composites in an Aerodynamic Profile,'' In: *Proceedings of SPIE 4698, Smart Structures and Materials 2002*, pp. 416–426.

Sivanesan, P., Sirkis, J.S., Murata, Y. and Buckley, S.G. 2002. ''Optimal Wavelength Pair Selection and Accuracy Analysis of Dual Grating Sensors for Simultaneously Measuring Strain and Temperature,'' *Optical Engineering*, 41(10):2456–2463.

Song, M., Lee, S.B., Choi, S.S. and Lee, B. 1997. ''Simultaneous Measurement of Temperature and Strain using Two Fiber Bragg Gratings Embedded in a Glass Tube,'' *Optical Fiber Technology*, 3(2):194–196.

Strang, G. 1988. *Linear Algebra and its Applications*, Harcourt Brace Jovanovich College Publishers, San Diego.

Wei, Z.G., Sandström, R. and Miyazaki, S. 1998a. ''Shape-memory Materials and Hybrid Composites for Smart Systems: Part I Shape-memory Materials,'' *Journal of Materials Science*, 33(15):3743–3762.

Wei, Z.G., Sandström, R. and Miyazaki, S. 1998b. ''Shape-memory Materials and Hybrid Composites for Smart Systems: Part II Shape-memory Hybrid Composites,'' *Journal of Materials Science*, 33(15):3763–3783.

Xu, M.G., Archambault, J.-L., Reekie, L. and Dakin, J.P. 1994. ''Discrimination between Strain and Temperature Effects using Dual-wavelength Fibre Grating Sensors,'' *Electronics Letters*, 30(13):1085–1087.

Yoon, H.J., Costantini, D., Michaud, V., Limberger, H.G., Månson, J.-A.E., Salathé, R.P., Kim, C.G. and Hong, C.S. 2005 ''*In-situ* Simultaneous Strain and Temperature Measurement of Adaptive Composite Materials using a Fiber Bragg Grating based Sensor,'' In: *Proceedings of SPIE 5758, Smart Structures and Materials 2005*, pp. 62–69.

Zeng, X.K. and Rao, Y.J. 2001. ''Simultaneous Static Strain, Temperature and Vibration Measurement using an Integrated FBG/EFPI Sensor,'' *Chinese Physics Letters*, 18(12):1617–1619.